Geometric Pathway to Scalable Quantum Sensing

Mattias T. Johnsson, Nabomita Roy Mukty, Daniel Burgarth, Thomas Volz, and Gavin K. Brennen*

*Center for Engineered Quantum Systems, Department of Physics and Astronomy, Macquarie University,
North Ryde, 2109 New South Wales, Australia*

Entangled resources enable quantum sensing that achieves Heisenberg scaling, a quadratic improvement on the standard quantum limit, but preparing large N spin entangled states is challenging in the presence of decoherence. We present a quantum control strategy using highly nonlinear geometric phase gates which can be used for generic state or unitary synthesis on the Dicke subspace with $O(N)$ or $O(N^2)$ gates, respectively. The method uses a dispersive coupling of the spins to a common bosonic mode and does not require addressability, special detunings, or interactions between the spins. By using amplitude amplification our control sequence for preparing states ideal for metrology can be significantly simplified to $O(N^{5/4})$ geometric phase gates with action angles $O(1/N)$ that are more robust to mode decay. The geometrically closed path of the control operations ensures the gates are insensitive to the initial state of the mode and the sequence has built-in dynamical decoupling providing resilience to dephasing errors.

Introduction.—Quantum enhanced sensing offers the possibility of using entanglement in an essential way to measure fields with a precision superior to that which can be obtained with unentangled resources [1–4]. Entangled resources allow the measurement sensitivity to scale as $1/N$ with respect to the resources applied (so-called Heisenberg scaling), compared to the $1/\sqrt{N}$ obtained otherwise (the standard quantum limit, or shot-noise limit) [4–6].

Creating large-scale entanglement in multipartite systems for the purposes of metrology is a difficult problem for a number of reasons. There is the difficulty in precisely constructing the required quantum state using realistic quantum operations, the need to protect that quantum state from decoherence and loss [7], and the problem of carrying out a number of quantum measurement operations on the state with precise control.

From a metrology perspective, there is also the issue that many schemes claim to achieve Heisenberg limit by virtue of quadratic scaling of the Fisher information of the system [8]. While this ensures that there is an observable which has an uncertainty that scales as $1/N$ with respect to some resource, it does not specify what that observable is, or require it be a convenient experimentally measurable quantity. There have been attempts to address these problems in various ways. For example, to mitigate the decoherence issue, recent work has suggested using quantum error correction assisted metrology (see Ref. [9], and references therein) or phase protected metrology [10]. Such workarounds require the ability to perform complex quantum control in the former case or engineered interactions in the latter.

Here we present a state preparation scheme and measurement protocol using geometric phase gates generalizing Ref. [11]. Our protocol addresses the issues of state preparation, decoherence protection, and choice of measurement operator. It is relatively simple to engineer as it involves only the coupling of an ensemble of qubits to a common bosonic mode, e.g., a cavity or mechanical oscillation, as well as simple global control pulses on the spins and mode. As such it is adaptable to a variety of architectures at the forefront of quantum control including nitrogen-vacancy (NV) centers in diamond, trapped ion arrays, Rydberg atoms, and superconducting qubits.

Unlike previous work our scheme does not require special engineering of the physical layout of the spins, special detunings for adiabatic state preparation, addressability, or direct interaction between the spins. Furthermore, it exceeds the performance of spin squeezing protocols because of the highly nonlinear nature of the geometric phase gates used. Another advantage is that due to the geometric nature of the gate, it is completely insensitive to variations or uncertainties in the rate at which the perimeter is traversed.

Furthermore, our protocol has dynamical decoupling built in, providing resilience against dephasing during the state preparation, which is the dominant source of noise in many physical implementations. While dynamical decoupling has been considered [12] in the context of the Møllmer-Sørenson geometric gate [13], our scheme extends this to a highly nonlinear geometric phase gate and a full quantum state preparation algorithm.

Method.—We consider a collection of two-level spin half systems, and define the collective raising and lowering angular momentum operators as $J^+ = \sum_{j=1}^{N} \sigma_j^+$, $J^- = (J^+)^\dagger$, and the components of the total angular momentum vector are $J^x = (J^+ + J^-)/2$,

$J^y = (J^+ - J^-)/2i$, $J^z = \sum_j(|0\rangle_j\langle 0| - |1\rangle_j\langle 1|)/2$. Dicke states are simultaneous eigenstates of angular momentum J and J^z: $|J = N/2, J^z = M\rangle$, $M = -J, ..., J$.

Consider the measurement of a field which generates a collective spin rotation about an axis perpendicular to $\hat{z}$ given by $U(\eta) = \exp[i\eta(J^x \sin\delta + J^y \cos\delta)]$. For a measurement operator O on the system, the single shot estimation of the parameter η has variance

$$(\Delta\eta)^2 = \frac{(\Delta O(\eta))^2}{|\partial_\eta\langle O(\eta)\rangle|^2}. \qquad (1)$$

When the measured observable is $O = J^{z2}$, the parameter variance is [14]

$$(\Delta\eta)^2 = [(\Delta J^{x2})^2 f(\eta) + 4\langle J^{x2}\rangle - 3\langle J^{y2}\rangle - 2\langle J^{z2}\rangle$$
$$\times (1 + \langle J^{x2}\rangle) + 6\langle J^z J^{x2} J^z\rangle][4(\langle J^{x2}\rangle - \langle J^{z2}\rangle)^2]^{-1},$$

with $f(\eta) = [(\Delta J^{z2})^2]/[(\Delta J^{x2})^2\tan^2(\eta)] + \tan^2(\eta)$. When the initial state is the Dicke state $|J, 0\rangle$, the estimate angle satisfies $\sin^2(\eta) = [8\langle J^{z2}(\eta)\rangle]/[N(N+2)]$ and the uncertainty in the measured angle is minimized at $\eta_{\min} = 0$ such that the quantum Cramér-Rao bound is saturated:

$$(\Delta\eta)^2 = \frac{2}{N(N+2)}. \qquad (2)$$

Note it is not essential that we know the angle δ of the field direction in the $\hat{x}$-$\hat{y}$ plane [15].

The best known quantum algorithm for deterministically preparing a Dicke state $|J, M\rangle$ requires $O((N/2 + M)N)$ gates and has a circuit depth $O(N)$ [16]. This works even for a linear nearest neighbor architecture, but requires a universal gate set and full addressability. Other proposals exist [17–20], but they all suffer from drawbacks such as not scaling beyond a few spins, strong adiabaticity or geometry, constraints, requiring large initial Fock states of motional modes, and couplings causing transitions outside the Dicke space.

In our setup we assume N spins with homogeneous energy splittings described by a free Hamiltonian $H_0 = \omega_0 J^z$ which can be controlled by semiclassical fields performing global rotations generated by J^x, J^y. Additionally, we assume the ensemble is coupled to a single quantized bosonic mode $\hat{a}$. Our scheme requires a dispersive coupling between the n spins and the bosonic mode of the form $V = ga^\dagger a J^z$.

The geometric phase gate (GPG) makes use of two basic operators [11,21], the displacement operator $D(\alpha) = e^{\alpha a^\dagger - \alpha^* a}$ and the rotation operator $R(\theta J^z) = e^{i\theta a^\dagger a J^z}$ which perform a closed loop in the mode phase space,

$$U_{\text{GPG}}(\theta, \phi, \chi) = D(-\beta)R(\theta J^z)D(-\alpha)R(-\theta J^z)$$
$$\times D(\beta)R(\theta J^z)D(\alpha)R(-\theta J^z)$$
$$= e^{-i2\chi\sin(\theta J^z + \phi)}, \qquad (3)$$

where $\phi = \arg(\alpha) - \arg(\beta)$ and $\chi = |\alpha\beta|$.

The system and the mode are decoupled at the end of the GPG cycle. Also, if the mode begins in the vacuum state, it ends in the vacuum state and the first operation $R(-\theta J^z)$ in Eq. (3) is not needed. In the GPG it is necessary to evolve by both $R(\theta J^z)$ and $R(-\theta J^z)$. This can be done by conjugating with a global flip of the spins $R(\theta J^z) = e^{-i\pi J^x}R(-\theta J^z)e^{i\pi J^x}$, implying that the GPG can be generated regardless of the sign of the dispersive coupling strength g. Furthermore, because $R(\pm\theta J^z)$ commutes with H_0 at all steps, this conjugation will cancel the free evolution accumulated during the GPG.

Assuming the number of spins n is even, we consider $N/2$ sequential applications of the GPG (see also Ref. [11]):

$$W(\ell) = \prod_{k=1}^{N/2} U_{\text{GPG}}(\theta_k, \phi_k(\ell), \chi)$$
$$= \sum_{M=-J}^{J} e^{-i2\chi\sum_{k=1}^{N/2}\sin(\theta_k M + \phi_k(\ell))}|J, M\rangle\langle J, M|,$$

with $\ell = 0, ..., N$.

$$\theta_k = \frac{2\pi k}{N+1}, \qquad \phi_k(\ell) = \frac{2\pi k(N/2 - \ell)}{N+1} + \frac{\pi}{2},$$
$$\chi = \frac{\pi}{N+1}$$

gives $W(\ell) = e^{-i\pi|J,\ell-N/2\rangle\langle J,\ell-N/2|}$, meaning it applies a π phase shift on the symmetric state with ℓ excitations. For N odd we can use N GPGs with the same angles $\theta_k, \phi_k(\ell)$ as above but with $\chi = \pi/2(N+1)$.

Given the control toolbox above of global rotations and the GPGs, one can synthesize an arbitrary unitary operator on the Dicke subspace. Writing $U = \sum_{k=1}^{N} e^{i\lambda_k}|\lambda_k\rangle\langle\lambda_k|$, where $\{|\lambda_k\rangle\}$ form an orthonormal basis on the Dicke subspace and $\lambda_k \in \mathbb{R}$ (note since the global phase is irrelevant we have set $\lambda_{2J+1} = 0$). This unitary can be decomposed as $U = \prod_{k=1}^{N-1}[K(\lambda_k)e^{i\lambda_k|J,-J\rangle\langle J,-J|}K^\dagger(\lambda_k)]$, where $K(\lambda_k)$ is any unitary extension of the state synthesis mapping $|J, -J\rangle \to |\lambda_k\rangle$. The phasing unitary is the same as $W(0)$ but with $\chi \to \lambda_k/(N+1)$. To construct $K(\lambda_k)$, we find the decomposition: $\tilde{K} = [\prod_{s=1}^{N-1} e^{i\beta_s J^y} U_{\text{GPG}}(\theta_s, \phi_s, \chi_s)]e^{-iJ^y(\pi/2)}U_{\text{GPG}}(\pi/2, 0, \pi/4)e^{iJ^y(\pi/2)}$ gives very accurate results when optimized over the $4N - 4$ free parameters $\{\beta_s, \theta_s, \phi_s, \chi_s\}$ [22]. The overall complexity in GPG count using this approach is N for state synthesis and $5N^2/2$ for unitary synthesis.

While the general state synthesis approach above can be used for building Dicke states, the $N - 1$ action angles $\{\chi_s\}$ that optimize state fidelity are $O(1)$ and this has implications for noise due to mode decay as described below. We now describe a way, based on amplitude amplification, to improve matters by only using the GPGs that appear in

$W(\ell)$ that have action angles $O(1/N)$, and with the added advantage of providing an analytical solution to the Dicke state synthesis problem. Starting with all spins down, i.e., in $|J, -J\rangle$, let the target state be $|w\rangle = |J, 0\rangle$. We will make use of the operators $U_w = e^{-i\pi|w\rangle\langle w|} = W(N/2)$ and $U_s = e^{-i\pi|s\rangle\langle s|} = e^{iJ^y\pi/2}W(0)e^{-iJ^y\pi/2}$. In total the operators U_w and U_s each use $N/2$ GPGs. The orbit of the initial state $|s\rangle$ under the operators U_w and U_s is restricted to a subspace spanned by the orthonormal states $|w\rangle$ and $|s'\rangle = (|s\rangle - |w\rangle\langle w|s\rangle)/\sqrt{1 - |\langle w|s\rangle|^2}$, exactly as in Grover's algorithm. The composite pulse is one Grover step $U_G = U_s U_w$. Geometrically, relative to the state $|s'\rangle$, the initial state $|s\rangle$ is rotated by an angle $\delta/2$ toward $|w\rangle$, where $\delta = 2\sin^{-1}(|\langle w|s\rangle|)$, and after each Grover step is rotated a further angle δ toward the target. The optimal number of Grover iterations to reach the target is $G = \lfloor \pi/4|\langle w|s\rangle| \rfloor$, where the relevant overlap is $\langle w|s\rangle = d^J_{-J,0}(\pi/2) = 2^{-J}\sqrt{(2J)!}/J!$. For $J \gg 1$ we have $\langle w|s\rangle \approx (\pi J)^{-1/4}$. Then the optimal number of Grover steps is

$$G = \lfloor \pi^{5/4}N^{1/4}/2^{9/4} \rfloor. \tag{4}$$

The fidelity overlap of the output state ρ of the protocol with the target state is $F = \text{Tr}(|w\rangle\langle w|\rho)$. For the Grover method it is easily calculated as

$$F = \sin^2[(G + 1/2)\delta] > 1 - \sqrt{2/\pi N}. \tag{5}$$

While the fidelity error falls off at least as fast as $\sqrt{2/\pi N}$ for all $N \gg 1$, if N is near a value where the argument in Eq. (4) is a half integer, i.e., $\lceil 32(2k + 1)^4/\pi^5 \rceil$, with $k \in \mathbb{Z}$, the error will be much lower. For example, at $N = (10, 70, 260, 700, 1552)$ the fidelity error is $(1.84\times10^{-4}, 1.57\times10^{-5}, 1.68\times10^{-6}, 3.65\times10^{-8}, 1.92\times10^{-8})$. The number of GPGs needed to prepare the Dicke state by the Grover method is $c \times N^{5/4}$ with a constant $c < 1$.

The effectiveness of our scheme when used for metrology is shown in Fig. 1, which shows the precision $\Delta\eta$ obtainable as a function of N, compared to that obtained from both the standard quantum limit and the ultimate Cramér-Rao bound. It also shows the fidelity obtainable as a function of the number of spins N. The achievable fidelity is clearly optimized for specific spin values.

We have focused on preparing the state $|J, 0\rangle$, but with simple modifications our protocol can prepare any Dicke state $|J, M\rangle$. First use the initial state $|s\rangle = e^{i\epsilon_M J^y}|J, -J\rangle$, and second substitute the operators $U_w = W(M + N/2)$ and $U_s = e^{i\epsilon_M J^y}W(0)e^{-i\epsilon_M J^y}$, where $\epsilon_M = \cos^{-1}(M/J)$. Now the relevant overlap is $|\langle w|s\rangle| = |d^J_{M,-J}(-\epsilon_M)|$, and for $J - |M| \gg 1$, $|d^J_{M,-J}(-\epsilon)| \approx (\sqrt{\pi J}\sin\epsilon_M)^{-1/2}$ [23], implying $G = O(N^{1/4})$.

Finally, measurement of J^{z2} could be done by again coupling the spins to the bosonic mode but now with a linear coupling $V_m = g_m J^z(a^\dagger + a)$ which generates a
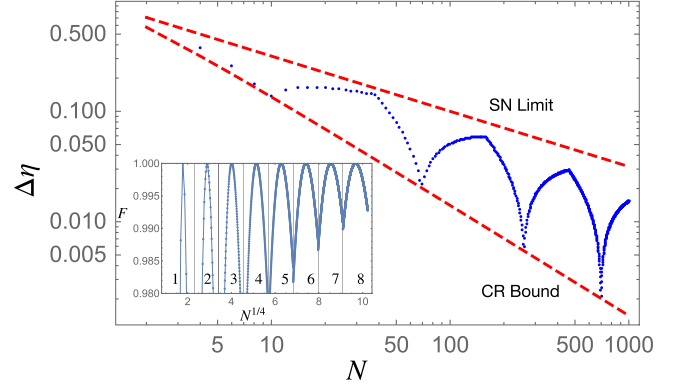

FIG. 1. Measurement precision $\Delta\eta$ as a function of number of spins (log-log scale). Shown are the shot-noise limit (upper red dashed line), the quantum Cramér-Rao bound given by Eq. (2) (lower red dashed line), and this protocol (blue). Inset: Fidelity for sets of ensemble sizes using the same number of Grover steps, which grow as $N^{1/4}$.

mode displacement depending on the collective spin projection. When the mode is in a number diagonal state, e.g., a thermal state, with mean excitation number $\bar{n}$, the measurement of $\hat{n}$ after a coupling time τ is $\langle \hat{n} \rangle = \bar{n} + (g_m\tau)^2\langle J^{z2} \rangle$. If mode number and quadratic spin operator measurements are difficult, there are alternatives. One is estimation by a classical average over p experiments: $E[\langle J^{z2} \rangle] = \sum_{k=1}^{p}(M(k)^2/p)$, where $M(k)$ is the outcome of the kth measurement of J^z [24]. Another is, after accumulating the signal, one could invert the state preparation and measure $|J, -J\rangle\langle J, -J|$ which gives the same precision scaling as Eq. (1), but does not require number resolved excitation counts.

There will be errors due to decay of the bosonic mode during the operations, as well as decoherence due to environmental coupling to the spins, which will degrade the fidelity. We now address these.

Mode damping.—We treat the mode as an open quantum system with decay rate κ. In order to disentangle the spins from the mode, the third and fourth displacement stages of the kth GPG should be modified to $D(-\alpha_k) \to D(-\alpha_k e^{-\kappa\theta_k/g})$ and $D(-\beta_k) \to D(-\beta_k e^{-\kappa\theta_k/g})$. For simplicity, we choose $|\alpha_k| = |\beta_k|$. For an input spin state in the symmetric Dicke space $\rho = \sum_{M,M'} \rho_{M,M'}|J, M\rangle\langle J, M'|$, the process for the kth GPG with decay on the spins, including the modified displacement operations above, is [25]

$$\mathcal{E}^{(k)}(\rho) = U_{\text{GPG}}(\theta_k, \phi_k, \chi_k)\left[\sum_{M,M'} R^{(k)}_{M,M'}\rho_{M,M'}|J, M\rangle\langle J, M'|\right]$$
$$\times U^\dagger_{\text{GPG}}(\theta_k, \phi_k, \chi_k),$$

where $\chi_k = |\alpha_k|^2 f(\theta_k)$, $f(\theta_k) = (e^{-3\theta_k\kappa/2g} + e^{-\theta_k\kappa/2g})/2$, and $\Gamma_{M,M'}$ and $\Delta_{M,M'}$ are given in the Supplemental Material [26].

The full operation is a concatenation of these imperfect processes $\mathcal{E}^{(k)}(\rho)$, and we characterize its accuracy with the process fidelity $F_{\text{pro}}(\mathcal{E}, U)$, which measures how close a quantum operation $\mathcal{E}$ is to the ideal operation U [28].

For each GPG we can readily find the lower bound on the process fidelity (see Supplemental Material [26]),

$$F_{\text{pro}}(\mathcal{E}, U_{\text{GPG}}) > e^{-6\pi\chi_k \kappa/f(\theta_k)g} \cos[\chi_k 4\pi\kappa/f(\theta_k)g].$$

Note the scaling of the exponent with $1/N$ since the action angles χ are $O(1/N)$. For the composite phasing map, numerically we find the tighter bound for the fidelity $F_{\text{pro}}(\mathcal{E}, W(\ell)) > e^{-\pi^2 \kappa/g}$, which is notably independent of N.

Dephasing.—We next address spin decoherence. We assume that amplitude damping due to spin relaxation is small by the choice of encoding. This can be accommodated by choosing qubit states with very long decay times either as a result of selection rules or by being far detuned from fast spin exchange transitions. Hence we will focus on dephasing. Because of the cyclic evolution during each GPG, there is error tolerance to dephasing because if the interaction strength between the system and environment is small compared to g, then the spin flip pulses used between each pair of dispersive gates $R(\theta a^\dagger a)$ will echo out this noise to low order.

For a given input density matrix $\rho(0)$, the output after a total time T has off-diagonal matrix elements that decay as $\rho_{M,M'}(T) = \rho_{M,M'}(0) e^{-(M-M')^2 A(T)}$. For the global dephasing map the numbers $M, M' \in [-N/2, N/2]$ are in the collective Dicke basis, while for local dephasing it is with respect to a local basis $M, M' \in [-1/2, 1/2]$. Our argument for suppression of dephasing works for both cases. Global dephasing is the most deleterious form of noise when the state has large support over coherences in the Dicke subspace, due to decay rates that scale quadratically in the difference in M number. However, it leaves the total Dicke space, and in particular the target Dicke state, invariant. Local dephasing induces coupling outside the Dicke space, but with a rate that is at most linear in N.

Consider the evolution during the $N/2$ control pulses to realize either of the phasing gates U_s or U_w. Assuming Gaussian bath statistics, the effective dephasing rate can be written as the overlap of the noise spectrum $S(\omega)$ and the filter function $|f(\omega)|^2$ [29,30]. As shown in the Supplemental Material [26], for our pulse sequence to lowest order in ω/g we find

$$g^2 |f(\omega)|^2 \approx \frac{(\omega/g)^2 \pi^4 N^2 (N+2)^2}{9(N+1)^2}. \tag{6}$$

Comparison with the case where no spin flips are applied is plotted in Fig. 2 showing there is substantial decoupling from the dephasing environment when the spectral density has dominant support in the range $\omega < g/2$.
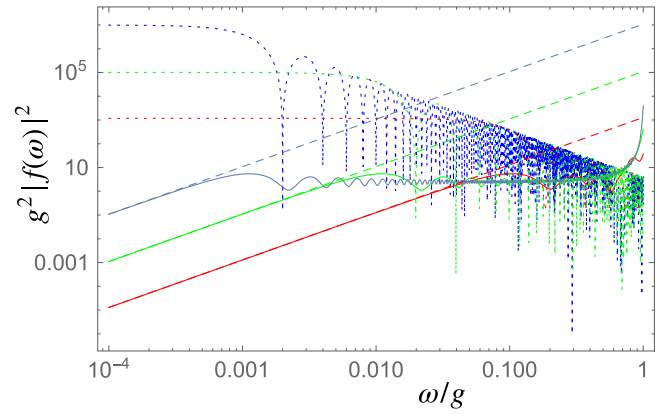

FIG. 2. Suppression of dephasing via dynamical decoupling inherent in the sequence of GPGs used for each of the operators U_s and U_w. Solid curves are filter functions using the GPGs. Dashed curves are plots of Eq. (6), which is a good approximation for $\omega/g < 1/\pi N$. Short dashed curves are the bare case without decoupling. Red, green, and blue curves correspond to $n = (10, 100, 1000)$ spins.

The freedom to apply the GPGs in any order allows for further improvement. Consider coupling to a zero temperature Ohmic bath with noise spectrum $S(\omega) = \alpha\omega e^{-\omega/\omega_c}$ with cutoff frequency $\omega_c/g = 0.1$. For $N = 20$, the ratio of the effective decay rate for the linearly ordered sequence of GPGs above to that with no decoupling is $A(T)/A_0(T) = 0.0085$. However, by sampling over permutations of the ordering of GPGs we find a sequence [31] achieving $A(T)/A_0(T) = 0.0026$. Examples of the effectiveness of our decoupling protocol on sensitivity for various values of $A(T)$ are shown in Fig. 3. Effectiveness on the fidelities can be found in the Supplemental Material [26].

Error-tolerant states.—The state preparation method we have described has inherent tolerance to decoherence. However, once the state is prepared further errors such as qubit loss or dephasing could accumulate. Strategies to address this by using superpositions of Dicke states were recently proposed [32]. The states considered were

$$|\varphi_u\rangle = \frac{1}{\sqrt{2^n}} \sum_{j=0}^{n} \sqrt{\binom{n}{j}} \left| J = \frac{knu}{2}, M = kj - J \right\rangle.$$

The number of spins $N = k \times n \times u$ and the parameters u and n determine the robustness of the states to some number of loss and dephasing errors, respectively. A state performing well in the presence of one erasure error is $u = 1, n = 2, k = N/2$, which can be written $|\varphi_1\rangle = \frac{1}{2}(|J, -J\rangle + \sqrt{2}|J, 0\rangle + |J, J\rangle)$ while $u = 2, n = 1, k = N/2$ tolerates one dephasing error and can be written $|\varphi_2\rangle = 1/\sqrt{2}(|J, -J\rangle + |J, 0\rangle)$. Both of these states can be prepared using our protocol. The specific steps are given in the Supplemental Material [26]. Superpositions of Dicke states also arise as code words of so-called permutationally invariant quantum codes [33], and of recently discovered
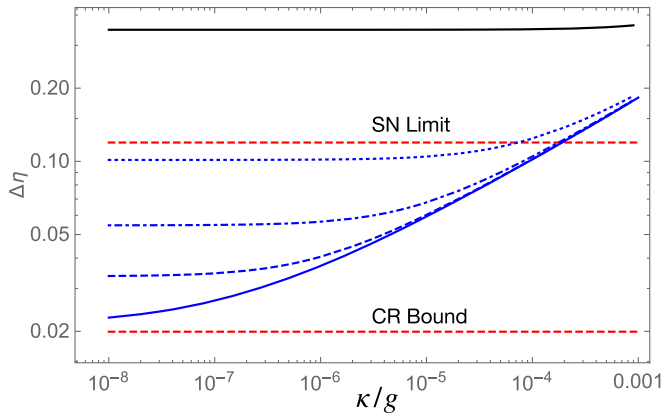
FIG. 3. Precision obtained for 70 spins with a single measurement of J^{z2} as a function of mode decay for various global dephasing factors $A(T)$: no global dephasing (blue line), $A(T) = 10^{-6}$ (blue dashed line), $A(T) = 10^{-5}$ (blue dot-dashed line), $A(T) = 10^{-4}$ (blue dotted line). These dephasings correspond to an underlying decoherence rate of $\gamma_{\mathrm{GDP}} = 10^{-4}g$ accumulated over each phasing gate of duration T. For a zero temperature Ohmic bath, the corresponding cuttoff frequencies are $\omega_c/g = \{0.003, 0.022, 0.094\}$. Black line shows performance without dynamical decoupling with $A_0(T) = 0.0223$.

codes which admit Gaussian Clifford operations [34] which our method could also prepare.

Implementations.—The scheme we have presented is amenable to a variety of architectures which allow collective dispersive couplings between spins and an oscillator. These include trapped Rydberg atoms coupled to a microwave cavity [35,36], trapped ions coupled to a common motional mode [37] or to an optical cavity mode [38], superconducting qubits coupled to microwave resonators [39], and NV centers in diamond coupled to a microwave mode inside a superconducting transmission line cavity [40].

One contender to test our scheme is Rydberg atoms coupled to microwave cavities. Recently the dispersive detection of small atomic Rydberg ensembles coupled to a high-Q microwave cavity was reported [36]. Their numbers suggest a ratio of $\kappa/g \approx 0.8$ (with $\kappa = 2\pi \times 11.8$ kHz and $g = 2\pi \times 14.3$ kHz). The collective coupling rate observed was a few megahertz, suggesting an additional pathway to improving γ/g by orders of magnitude by encoding spins through collective subensembles. Consider an encoding where each spin is composed of n physical spins with logical states $|0\rangle = |j = n/2, -j\rangle$ and $|1\rangle = |j = n/2, -j + 1\rangle$, i.e., the permutationally invariant states of zero or one excitation shared among the n spins. If the spins within each logical qubit interact, e.g., via dipole-dipole interactions, there will be a dipole blockade to larger numbers of excitations. Hence, collective rotations frequency tuned to the transition energy $E_1 - E_0$ will be collective but only act on this qubit subspace. The dispersive interaction strength is enhanced by $g \to g\sqrt{n}$,

provided the number n is similar for all logical spins. Using this kind of encoding, dispersive coupling with strength $g \approx 2\pi \times 2.2$ MHz was obtained with NV ensembles in diamond bonded onto a transmission line resonator with quality factor $Q \approx 4300$ at the first harmonic frequency $\omega_1 = 2\pi \times 2.75$ GHz. Microwave cavities with much higher quality factors, e.g., $Q \approx 10^9$, have been realized [41], which for the same dispersive coupling could provide $\kappa/g \approx 10^{-6}$.

*gavin.brennen@mq.edu.au
[1] W. Wasilewski, K. Jensen, H. Krauter, J. J. Renema, M. V. Balabas, and E. S. Polzik, Phys. Rev. Lett. **104**, 133601 (2010).
[2] J. Taylor, P. Cappellaro, L. Childress, L. Jiang, D. Budker, P. R. Hemmer, A. Yacoby, R. Walsworth, and M. D. Lukin, Nat. Phys. **4**, 810 (2008).
[3] W. Wang et al., Nat. Commun. **10**, 4382 (2019).
[4] V. Giovannetti, S. Lloyd, and L. Maccone, Nat. Photonics **5**, 222 (2011).
[5] V. Giovannetti, S. Lloyd, and L. Maccone, Science **306**, 1330 (2004).
[6] S. Pirandola, B. R. Bardhan, T. Gehring, C. Weedbrook, and S. Lloyd, Nat. Photonics **12**, 724 (2018).
[7] R. Demkowicz-Dobrzański, J. Kołodyński, and M. Guţă, Nat. Commun. **3**, 1063 (2012).
[8] M. Zwierz, C. A. Pérez-Delgado, and P. Kok, Phys. Rev. Lett. **105**, 180402 (2010).
[9] S. Zhou, M. Zhang, and L. Jiang, Nat. Commun. **9**, 78 (2018).
[10] S. D. Bartlett, G. K. Brennen, and A. Miyake, Quantum Sci. Technol. **3**, 014010 (2017).
[11] X. Wang and P. Zanardi, Phys. Rev. A **65**, 032327 (2002).
[12] G. Xu and G. Long, Phys. Rev. A **90**, 022323 (2014).
[13] A. Sørensen and K. Mølmer, Phys. Rev. Lett. **82**, 1971 (1999).
[14] I. Apellaniz, B. Lücke, J. Peise, C. Klempt, and G. Tó, New J. Phys. **17**, 083027 (2015).
[15] This follows from $U(\eta) = \exp[i\eta(J^x \sin \delta + J^y \cos \delta)] = \exp(i\delta J^z)\exp(i\eta J^y)\exp(-i\delta J^z)$, the fact our measurement observable is $\hat{J}^{z2}$, and our initial state is $|J, M = 0\rangle$.
[16] A. Bärtschi and S. Eidenbenz, arXiv:1904.07358.
[17] C. Wu, C. Guo, Y. Wang, G. Wang, X.-L. Feng, and J.-L. Chen, Phys. Rev. A **95**, 013845 (2017).
[18] K. D. B. Higgins, S. C. Benjamin, T. M. Stace, G. J. Milburn, B. W. Lovett, and E. M. Gauger, Nat. Commun. **5**, 4705 (2014).
[19] T. Keating, C. H. Baldwin, Y.-Y. Jau, J. Lee, G. W. Biedermann, and I. H. Deutsch, Phys. Rev. Lett. **117**, 213601 (2016).

[20] D. B. Hume, C. W. Chou, T. Rosenband, and D. J. Wineland, Phys. Rev. A **80**, 052302 (2009).

[21] L. Jiang, G. K. Brennen, A. V. Gorshkov, K. Hammerer, M. Hafezi, E. Demler, M. D. Lukin, and P. Zoller, Nat. Phys. **4**, 482 (2008).

[22] This was tried for up to $N = 100$ spins with the decomposition having fidelity error $1 - |\langle \lambda | \tilde{K} | J, -J \rangle|^2 < 10^{-12}$ for synthesizing sampled random state vectors $|\lambda\rangle$.

[23] D. J. Rowe, H. de Guise, and B. C. Sanders, J. Math. Phys. (N.Y.) **42**, 2315 (2001).

[24] B. Lücke *et al.*, Science **334**, 773 (2011).

[25] G. K. Brennen, K. Hammerer, L. Jiang, M. D. Lukin, and P. Zoller, arXiv:0901.3920.

[26] See Supplemental Material at http://link.aps.org/supplemental/10.1103/PhysRevLett.125.190403 for details. The Supplemental Material contains a derivation of the gate fidelity in the presence of mode decay, calculations for $\Gamma_{M,M'}$ and $\Delta_{M,M'}$, and the calculation of the process fidelity. It also includes the derivation of the filter functions, as well as an explicit example of a quantum circuit to prepare the error tolerant states, which includes Ref. [27].

[27] G. K. Brennen, G. Pupillo, E. Rico, T. M. Stace, and D. Vodola, Phys. Rev. Lett. **117**, 240504 (2016).

[28] M. Nielsen and I. L. Chuang, *Quantum Computation and Quantum Information* (Cambridge University Press, Cambridge, England, 2010).

[29] G. S. Agarwal, Phys. Scr. **82**, 038103 (2010).

[30] Z.-Y. Wang and R.-B. Liu, *Quantum Error Correction* (Cambridge University Press, Cambridge, England, 2013), pp. 351–375.

[31] The ordering $\{8, 4, 5, 9, 3, 7, 6, 2, 10, 1\}$ achieves this. Note an exhaustive search over all 10! permutations was not done.

[32] Y. Ouyang, N. Shettell, and D. Markham, arXiv:1908.02378.

[33] H. Pollatsek and M. B. Ruskai, Linear Algebra Appl. **392**, 255 (2004).

[34] J. A. Gross, arXiv:2005.10910.

[35] C. Sayrin *et al.*, Nature (London) **477**, 73 (2011).

[36] S. Garcia, M. Stammeier, J. Deiglmayr, F. Merkt, and A. Wallraff, Phys. Rev. Lett. **123**, 193201 (2019).

[37] J. S. Pedernales, I. Lizuain, S. Felicetti, G. Romero, L. Lamata, and E. Solano, Sci. Rep. **5**, 15472 (2015).

[38] M. Lee, K. Friebe, D. A. Fioretto, K. Schüppert, F. R. Ong, D. Plankensteiner, V. Torggler, H. Ritsch, R. Blatt, and T. E. Northup, Phys. Rev. Lett. **122**, 153603 (2019).

[39] C. Wang *et al.*, Science **352**, 1087 (2016).

[40] T. Astner, S. Nevlacsil, N. Peterschofsky, A. Angerer, S. Rotter, S. Putz, J. Schmiedmayer, and J. Majer, Phys. Rev. Lett. **118**, 140502 (2017).

[41] A. R. Castellia, L. A. Martinez, J. M. Pate, R. Y. Chiao, and J. E. Sharping, J. Appl. Phys. **126**, 173908 (2019).